Improving Depth Averaged Velocity Measurements from Seaglider with an Advanced Acoustic Current Profiler, the Nortek AD2CP-Glider

Peter J Rusello
NortekUSA
Boston, MA 02125
Email: pj@nortekusa.com

Christopher Yahnker
and Mark Morris
iRobot Corporation
4625 Industry Lane
Durham, NC 27713
Email: cyahnker@irobot.com, mmorris@irobot.com

***Abstract*—Autonomous underwater gliders offer a unique sampling platform for ocean measurements with a variety of sensors. A fundamental problem with gliders (and other autonomous underwater vehicles) is locating measurements within the water column with reasonable horizontal and vertical accuracy. Underwater positioning systems, generally based on acoustic travel time, can provide reasonable accuracy but slow update rates because of the acoustic path length. The slow update rate is problematic when dynamic environmental conditions exist such as near the surface. These systems are also unsuited to adaptive sampling strategies or the kilometers long transect lines gliders often fly. Dead reckoning navigation is an ancient technique relying on estimates of speed and direction to propagate an initial position fix forward in time until a new position fix is obtained. Recent work between iRobot and Nortek has resulted in the integration of a next generation acoustic velocity profiler, the AD2CP-Glider, into the iRobot® 1KA Seaglider™. The relative velocities measured by the AD2CP-Glider are used to improve dead reckoning position estimates throughout the water column and predict the location of the glider on surfacing based on an initial position fix obtained via GPS at the start of a dive cycle. Error sources, such as surface drift, are identified and corrected for when possible. Data from tests in a large lake are used to assess the validity of the dead reckoning navigation. Depth averaged velocity estimates derived from the dead reckoned navigation are compared to estimates obtained using a hydrodynamic model to predict glider velocity. The measurement based estimates are expected to perform better in more complex flows where the interaction between the flow and glider is not captured by the hydrodynamic model.**

I. Introduction

The iRobot® 1KA Seaglider™, is a long-range, high endurance autonomous underwater vehicle (AUV) that is used for a wide variety of oceanographic studies. Developed by the University of Washington with funding from the U.S. Office of Naval Research and the National Science Foundations, Seaglider is able to perform a wide range of data collection missions in environments as shallows as 50 meters diving up to 1,000 meters. Operating for months and covering thousands of nautical miles, Seaglider gathers data that aids in the scientific discovery and the understanding of the physical properties of the world's oceans.

One significant challenge with data from glider mounted sensors is knowing where data was collected once the glider leaves the surface. Through the use of pressure sensors, the vertical position of a glider in the water column is easily obtained with high accuracy (typically 0.1% of the pressure sensor full scale). However, once the glider leaves the surface, there is a lack of accurate horizontal position data that can lead to mis-interpretation of where sensor data was collected. This also means there is no reference for velocity data to express it as an absolute rather than relative measurement.

In some cases, a dive may occur over a time and spatial scale small enough to represent a snapshot of the ocean at that time and location. In other cases, the time and spatial scales may be large enough they encompass a variety of conditions or forcings. The lack of horizontal position data can lead to data mis-interpretation when conditions vary along a dive path. This can also result in error propagation to related data products like model ocean forecasts. Accurate position information is important in interpreting observations made from ocean gliders, especially over large spatial and temporal scales.

Dead reckoning navigation is a simple method to estimate position. It relies on estimates of speed and direction to propagate a known position forward in time until a new position fix is obtained. Dead reckoning is subject to integration errors, where a small initial error over time leads to a large error in position. Despite this shortcoming, it is ideally suited to autonomous gliders where no external reference for horizontal location is available once the glider has left the surface, but good estimates of glider velocity and heading are available.

Nortek and iRobot have worked together on the integration of a next generation Doppler current profiler, the AD2CP-Glider, into the science payload of the iRobot Seaglider. While the ultimate goal of this ongoing collaboration is to obtain absolute water velocity profiles, an important benefit of the integration, coupled with surface GPS positions and pressure measurements, is an improvement in dead reckoned navigation and determining the glider horizontal position. This improved localization, in addition to providing position information for

other measurements, provides an improvement in the depth averaged velocity ($\overline{U}$) by reducing the assumptions made when calculating an approximate glider path.

II. Velocity Measurements and Depth Averaged Velocities

In a quiescent ocean, the velocities measured by the AD2CP-Glider will be exactly the glider velocity through the water and over the ground.

$$V_m(t_i, z_0 + r) = -V_g(t_i, z_0) \tag{1}$$

Where $V_m(t_i, z_0 + r)$ is the measured velocity, $V_g(t_i, z_0)$ is the glider velocity at time t_i, z_0 is the glider depth, and r are the ranges to the measurements cells in the velocity profile.

A glider launched at Point A (x_a, y_a) and recovered at Point B (x_b, y_b) could be tracked on its path between these points by integrating the velocity record from the profiler regardless of path complexity. Any errors in this path would be due to the measurement noise or the discretization of the velocity (i.e. a more exact path could be determined by sampling faster).

With the addition of a mean, potentially depth and time varying, current $(V_w(t_i, z_0 + r)$ the velocity profiler measurements are now the relative velocity between the glider and the water.

$$V_m(t_i, z_0 + r) = -V_g(t_i, z_0) + V_w(t_i, z_0 + r) \tag{2}$$

Assuming the glider travels exactly with the mean velocity at its depth, the glider velocity can be expressed as

$$V_g(t_i, z_0 + r) = V'_g(t_i, z_0) + V_w(t_i, z_0) \tag{3}$$

Where $V'_g(t_i, z_0)$ is the glider velocity in a quiescent ocean. Substituting Eqn. 3 into Eqn.2 yields

$$V_m(t_i, z_0{+}r) = -V'_g(t_i, z_0){+}[V_w(t_i, z_0{+}r){-}V_{t_i,wi}(z_0)] \tag{4}$$

The glider path between Points A and B is not known exactly with the addition of a mean current because the glider velocity is now modified by the local water velocity and the measurements are a combination of the water and glider velocity. In many flows, the glider forward velocity will be much larger than the velocity difference term on the right hand side of Eqn. 4. This means the measured velocity will be a good approximation of the glider velocity. A similar argument holds true for the vertical velocity, which will be dominated by the glider's descent or ascent rate. The glider's lateral velocity is typically assumed zero, but in the presence of a lateral flow component will be non-zero and difficult to measure (similar to leeway for a sailboat).

Equations 2 and 4 describe the relative velocity measurements in two different ways. In 2 the glider velocity is explicitly its speed over ground needed to propagate a known position fix forward in time. In 4, the glider velocity is described as its ideal velocity in a quiescent ocean, such as would be obtained from a hydrodynamic model. This equation provides a means to estimate shear profiles at various length scales without the need to numerically differentiate the data.

Eqn. 2 serves as the basis for depth averaged velocity estimates from measurements. As initially presented, the measurements are a function of the vertical coordinate, z, and time t. If we assume the velocities are independent of the vertical coordinate z, the local water velocity $(V_w(t_i, z_0 + r))$ can be replaced by the depth averaged velocity $\overline{U}$ (also assumed independent of time over the dive) and $V_g(t_i, z_0)$ with a depth averaged glider velocity ($\overline{V_g(t_i)}$, not independent of time, in Equation 2, removing the dependence on z from V_m. This results in

$$V_(m)(t_i) = -\overline{V_g(t_i)} + \overline{U} \tag{5}$$

Integrating this equation in time yields the depth averaged velocity

$$\overline{U_w} = \frac{1}{T}\left(\int_0^T V_m(t_i)dt + \int_0^T V_g(t_i)dt\right) \tag{6}$$

Where the term $\int_0^T V_g(t_i)dt$ is known from an external reference system such as GPS (with multiplication by -1 to account for the change in frame of reference). This depth averaged velocity represents a temporal average over some time period, T, equal to the total observation period or time underwater, and a path average along the glider's path. The interpretation of this depth averaged velocity is dependent on specific flow and environmental conditions. Another estimate of $\overline{U}$ is obtained by treating Eqn. 3 in a similar manner, where the V'_g term is estimated from a hydrodynamic model of glider flight [1].

III. Dead Reckoning Navigation

Dead reckoning accuracy depends primarily on the accuracy of the initial position fix, the accuracy of velocity estimates, and the accuracy of the heading used to propagate this position forward in time. The AD2CP velocity magnitude accuracy is specified as 0.5% of the measured value, $\pm$ 1 mm/s. The compass accuracy is specified as $\pm 2^\circ$.

The errors in both velocity and heading can be grouped into random and bias errors. For acoustic Doppler systems, the random errors (also called the Doppler noise) can be assumed independent of the measurements with characteristics of white noise [2]. By propagating a position forward in time over a long enough period, this error source is in effect averaged out. Random errors will introduce uncertainty into individual position estimates but minimal error to the overall path obtained by integrating the velocity.

Bias errors, such as introduced by an incorrect speed of sound, are a concern, because they will grow with time (i.e. they do not integrate to zero). A 1-2% error in speed of sound will translate directly into a 1-2% error in final position. The difference between the measured and actual glider velocity can also be thought of as a bias error, however in this case, the source of this bias is known (or at least assumed known) and is a quantity of interest, the depth averaged velocity.

A physical rotation between the instrument axes and the glider axes will introduce a bias in velocities, resulting in a minor, but again cumulative error in position. This rotation is expected to be $\pm 2^\circ$. If the internal compass of the AD2CP is assumed perfectly aligned with the instrument axes, and similarly Seaglider's compass is perfectly aligned with the glider axes, this offset should show up as a constant offset in the heading values between the two instruments.

The heading is also subject to random and bias errors. The random error is expected to be both fairly small and behave similarly to the Doppler noise terms for velocity measurements (i.e. as white noise). Because the heading reported is an ensemble of multiple readings, the random error in the compass is expected to be small in comparison to bias errors.

Hard and soft iron effects are the most common source of bias in compass readings. Currently this bias is minimized by simultaneously calibrating Seaglider's compass and the AD2CP internal compass, which should also provide an estimate of any potential offset between the two compasses. The specified accuracy of the heading ($\pm 2^\circ$) is unfortunately not uniform around a circle. An additional complication is the large pitch and roll angles of the glider, which necessitates accurate tilt measurements to correct the compass measurements. This means depending on the direction the AD2CP is facing and its orientation to gravity, there could be a larger bias error than if the heading were 90° to port or when the glider is ascending or descending.

While all of these errors are fairly small, taken together they can create a larger error and higher uncertainty in the dead reckoned positions. Because the magnitude of most of these errors is known, they can be incorporated into dead reckoning calculations to obtain a cone of uncertainty around the true glider path.

A. Initial Position Fix

At the start and end of a dive, Seaglider obtains a position estimate using GPS. These position estimates can occur approximately 2-3 minutes before or after Seaglider leaves or reaches the surface (top panel Figure 1). Occasionally, much longer times occur at the end of a dive as GPS satellites take longer to acquire. During this time, the glider position can change considerably, depending on surface conditions such as the sea state or wind speed.

Calculating an average surface drift velocity from the previous dive's end of dive position estimate and the current dive's start of dive position estimate is straightforward (bottom panel Figure 1). By using the time between the GPS position report and when the glider leaves or returns to the surface, corrected start and end positions are determined. While not currently used, the horizontal dilution of precision reported by the GPS could be used to describe a probable region where the glider is located at the time of the GPS position fix. For longer duration dives, it is advisable to use different drift velocities calculated from the previous and current dive's end and start positions and the current and next dive's end and start positions.

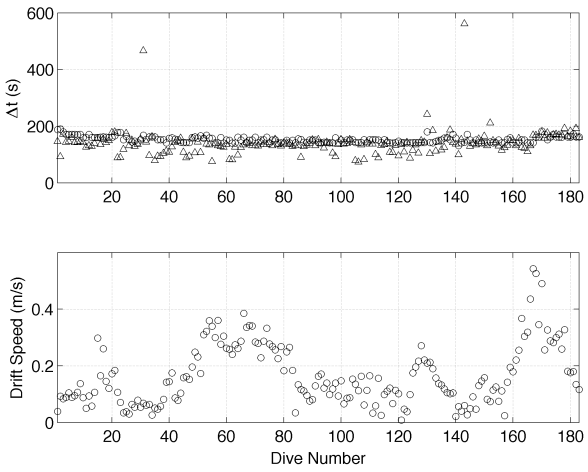

Fig. 1. (top)Time difference between start of dive GPS position and the glider leaving the surface (○) and the glider return to the surface and end of dive GPS position (△). (bottom) Surface drift velocities in a large lake.

It is straightforward to estimate a displacement vector using the measured or hydrodynamic model velocities, sample interval and expected heading errors. While there are other potential error sources mentioned above, the heading error tends to dominate uncertainty in position [3]. In conjunction with the initial position estimate, the estimated displacement vectors provide dead reckoned position estimates at each sample time for the AD2CP-Glider and interpolated positions when asynchronous sampling occurs with other sensors.

B. Measured Velocities and Coordinate Systems

The AD2CP-Glider operates at 1 MHz and uses an asymmetric four beam head, with two pairs of opposing beams (Figure 2. The fore and aft beams (numbered 1 & 3) have a larger angle from the instrument z-axis (a small angle from the x-y plane) than the port and starboard (numbered 2 & 4) beams. When the glider nose is pitched down during the descent phase of a dive, the forward, port and starboard beams (beams 1, 2 and 4) form a symmetric three beam system (Figure 3). Similarly, the aft, port and starboard beams (beams 2, 3, and 4) form a symmetric three beam system when the glider is ascending.

Like all mono-static Doppler current profilers, the AD2CP-Glider measures radial velocities along its four acoustic beams (Figure 4). By using a coded pulse phase determination algorithm, single ping data from a pre-production system shown in Figure 4 provides low-noise velocity measurements. The 1 MHz operating frequency provides an approximately 20 m range, subdivided here into 2 m long range cells. Low scattering occasionally affects the farthest bins, visible as darker patches in the last few bins. Bottom reflections cause the speckled pattern from 800-1200 seconds.

Linear combinations of the beam velocities are used to isolate velocities of interest such as East, North and Up. The three beam systems are used to calculate forward, lateral

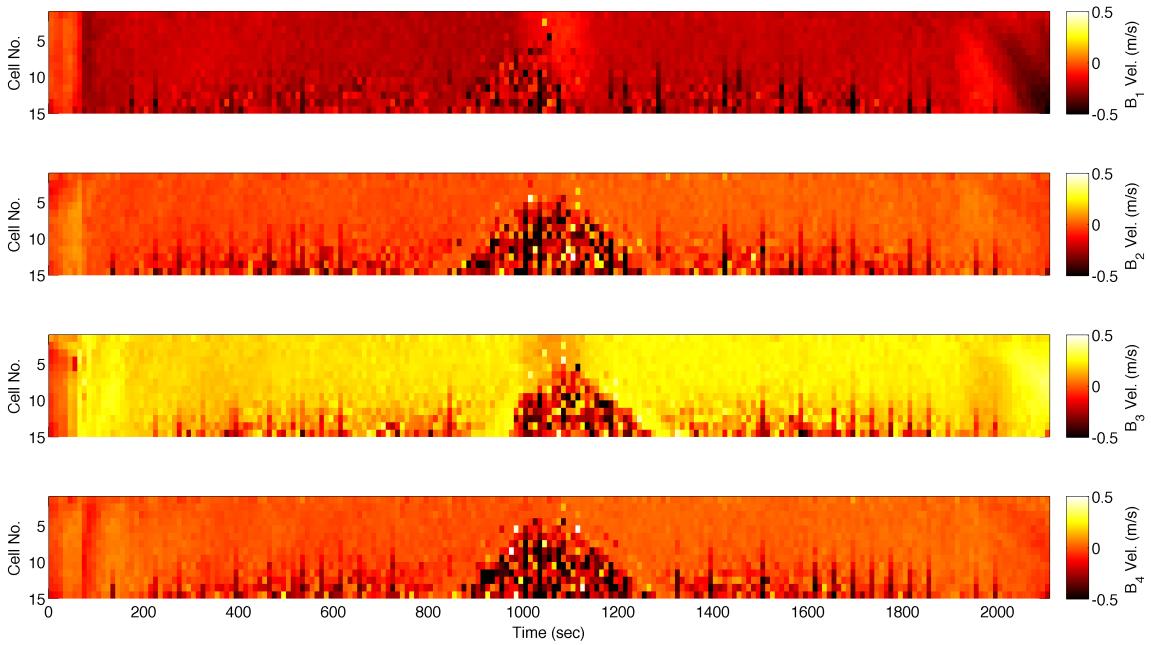

Fig. 4. Example beam velocities from the AD2CP glider (beams 1-4, top to bottom).

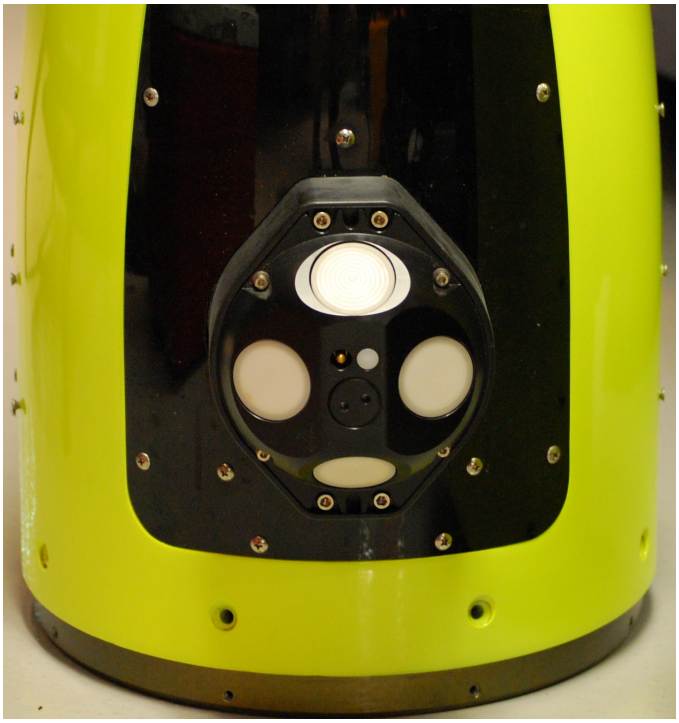

Fig. 2. The AD2CP-Glider mounted in the aft fairing of Seaglider. Beam 1 is at the bottom, beam 2 is to its right.

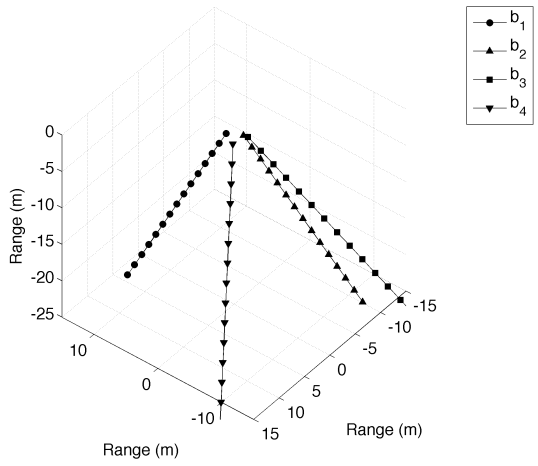

Fig. 3. Beam mapping for a pitch angle of -17.4° during descent.

and vertical velocities for the glider using an appropriate transformation matrix [4].

Forward is in the direction of the glider's nose but perpendicular to gravity, lateral is positive to port and perpendicular to gravity and vertical is parallel with gravity, positive towards the free surface. Corrections for pitch and roll are applied as needed. Pitch angles, while often exceeding 20° in magnitude, are typically less than 5° in practice during descent and ascent because of the orientation of the three beam system's profile axis relative to the glider's pitch axis, an approximately 17° offset (see Figure 3).

There are three regions where coordinate transformations bear further consideration. These are the regions near the

surface where the glider is not on an optimal glide path at the start and end of a dive and at the transition between descent and ascent when the glider reaches its lowest point (Figure 5).

At the start of a dive, in order to quickly clear the surface and achieve its glide path, Seaglider takes on a steep pitch angle till it reaches its flare depth (D_FLARE) where it levels out to the commanded pitch angle. At the end of a dive, when D_SURF is reached, Seaglider begins to level out as it nears the surface before assuming an extremely steep pitch angle to expose its antenna for communications and GPS acquisition. While relatively short duration, these two periods and the region of the water column where they occur are characterized by strong velocities, waves, wind effects, and suboptimal glider performance. In particular, the wings of the glider will be oriented almost perpendicular to the flow, greatly increasing drag and thus drift velocity. Surface contamination of the AD2CP-Glider can also occur (particularly in Beam 3 pointing aft).

The transition region between descent and ascent (the dive apogee) can last two to four minutes depending on the programmed thrust of the glider and the pump rate of the glider buoyancy engine. In this region, the pitch is near zero so the three beam systems used during descent and ascent are in effect exposed to large pitch angles greater than 10°. During these periods, the three beam geometry is less appropriate and alternate transformations can be used.

The simplest is to use opposing beam pairs to isolate two velocity components as typically done with a four beam system [5]. These two beam transformations result in instrument XYZ velocities which are aligned with the positive X-axis in the direction of the glider nose, the Y-axis pointing to port and the Z-axis pointing towards the top of the glider body (i.e. toward the free surface but at an angle from vertical equal to the current pitch). Rotating the XYZ velocities into forward lateral and vertical velocities is accomplished using the reported pitch and roll values, which during this period tend to be less than 10°.

These two beam transformations can also be used during the descent and ascent phases of the dive, but because of the opposing beam's geometry and the large pitch angles, one beam of the fore/aft pair will sample at different vertical locations (the classic beam mapping problem) and thus will measure a different combination of water and glider velocity assuming there is vertical structure in the water column. In many flows, this difference will be negligible as the largest component of the measured velocity will be due to the glider's motion. During certain periods or pitch conditions, other possible beam mappings may be used, including one beam solutions to estimate a velocity component directly.

Example time series of the forward, lateral and vertical velocities are shown in Figure 6 obtained with both the three beam and two beam solutions. An estimate of the glider horizontal velocity from the hydrodynamic model is plotted alongside the measured values [1]. Also plotted for the vertical component is an absolute estimate of glider vertical velocity obtained from $\frac{dP}{dt}$. The time when Seaglider leaves the surface and returns to the surface are marked by vertical lines. The measured velocities represent an average of five, 2 m long range cells.

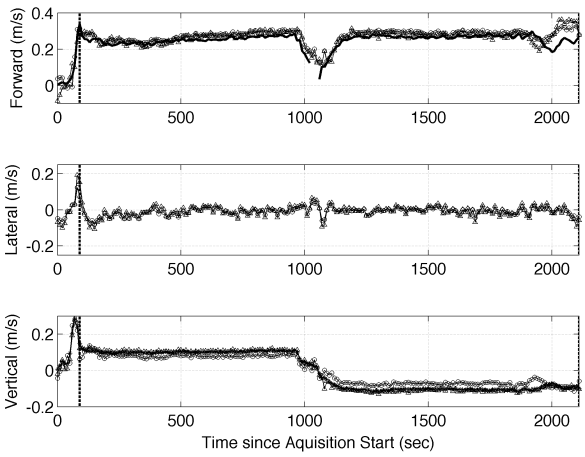

Fig. 6. Forward, lateral, and vertical velocities measured by the AD2CP-Glider during a dive. Two beam solutions (○) and three beam (△) solutions are plotted for all three components. The hydrodynamic model forward velocity (–) and $\frac{dP}{dt}$ (∗) are plotted for the forward and vertical components.

As discussed above, agreement between the two beam and three beam velocity estimates during the descent and ascent portions of the dive is quite good. The root-mean-square (RMS) difference between the estimates during the constant pitch regions characterizing descent and ascent are 0.018, 0.011 and 0.036 m/s for the plotted, typical of data for this deployment. The higher value for the vertical RMS difference is likely due to the pitch corrections applied, where the two beam systems see significantly larger relative pitch values than the three beam systems.

Agreement between the hydrodynamic model and measured forward velocities is good in general form and in magnitude. The RMS difference between the two in Figure 6 is 0.04 m/s, which is primarily due to the water velocity and provides a rough estimate for the magnitude of the depth averaged velocity. This estimate will be biased by the glider heading relative to the mean current however. Lateral velocities are near zero as expected, but not exactly zero. This is a result of both the weak velocities where these measurements were made, measurement noise, imperfect beam mappings, and the tendency of the glider to move with any cross flow at the same speed. The three beam solution agrees better with the vertical velocity estimate obtained from $\frac{dP}{dt}$, with an RMS difference of 0.010 m/s, compared to an RMS difference of 0.030 m/s for the two beam solution. The larger difference for the two beam solution is attributable to the larger pitches seen by the two beam systems and different vertical locations for these beams. These differences are typical of all dives.

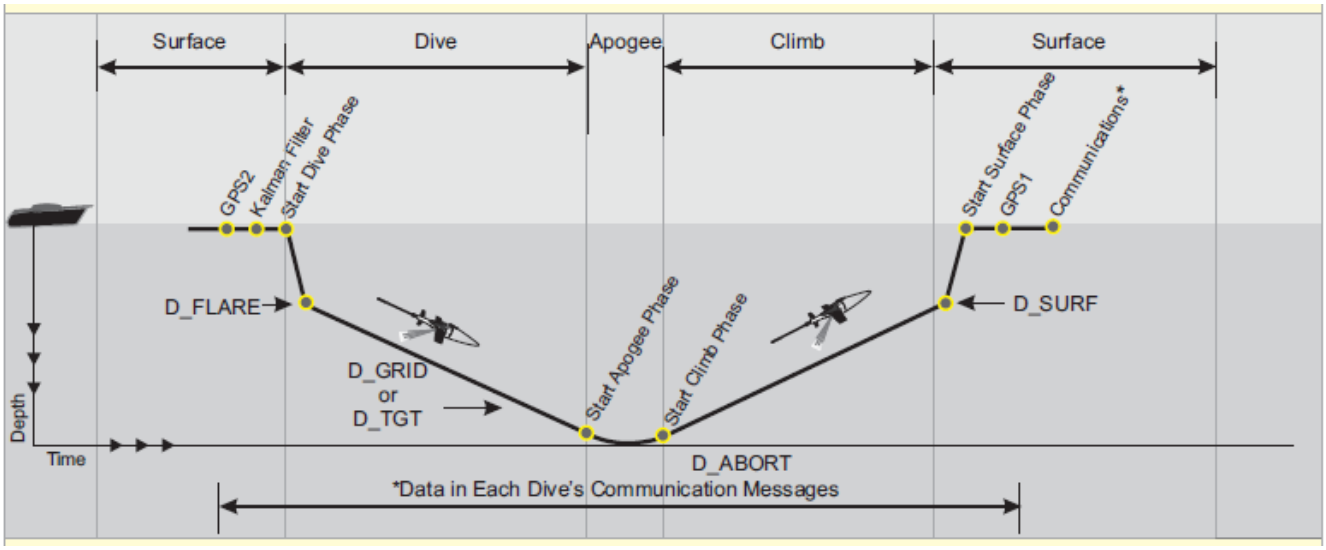

Fig. 5. An example dive profile for Seaglider with important regions indicated.

C. Glider Tracks

The approximate glider path is generated by a stepwise integration of the three beam system velocity time series, switching between Beams 1, 2, & 4 and Beams 2, 3, & 4 at the maximum depth. The corrected for surface drift starting point is the initial position. A separate track is made by integrating the hydrodynamic model estimated velocity time series. Any gaps in a time series are filled by using the last known valid velocity estimate until a new valid velocity estimate is available. A typical gap lasts 30-60 seconds and generally occurs when Seaglider comes too close to the bottom for valid measurements or at pitch angles where the hydrodynamic model is not valid. Measurements and model velocities are decomposed into East and North components using the reported heading, with a $\pm 2^{\circ}$ uncertainty applied to heading to obtain bounds on the estimated position. An example Seaglider track is shown in Figure 7. All locations have been referenced to the uncorrected initial position at $(0, 0)$.

The example paths agree well in shape since they are using the same heading. Difference in path length is related to what the two estimates of the glider velocity assume. The measured velocity is a combination of the glider and water velocity while the model velocity is an estimate of the glider velocity only. The measured path also incorporates the lateral velocity component, which despite being near zero, over time will cause an appreciable separation in the paths.

The example dive is fairly simple, with only one turn near the start. Separation between the two paths is minimal because of the short duration of the dives (approximately 30 minutes in this case). A dive with multiple turns and a longer duration would result in a larger separation between the paths. While constrained by other considerations such as power and a need to minimize surface time, minimizing the time between position fixes from the GPS is desirable to keep error growth in check. Note that dive duration and path complexity will have minimal effect on depth averaged velocity estimates because the error is now normalized per unit time.

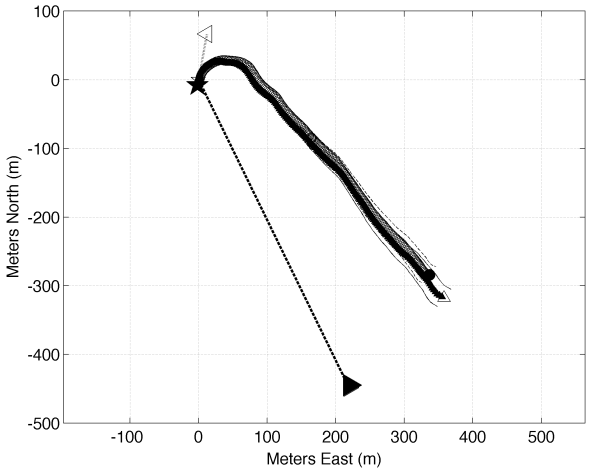

Fig. 7. Example glider paths using velocities measured by the AD2CP-Glider and estimates of glider velocity obtained using a hydrodynamic model during a dive. The measured velocity path is shown by $\triangle$ while the hydrodynamic model path is shown by ($\bullet$). The corrected start position is shown by a filled $\star$ with the initial reported position an unfilled $\star$. The previous dive surface drift position is marked by $\triangleleft$. The corrected and reported end position is marked by filled and unfilled $\triangleright$. Light solid and dashed lines mark the envelope of positions the glider could occupy by accounting for uncertainty in heading.

IV. Depth Averaged Velocities

A test deployment of the AD2CP-Glider installed on an iRobot Seaglider was conducted in June 2012 in Cayuga Lake in New York State. Cayuga Lake is a large monomictic lake and part of the Finger Lakes of New York. It is approximately 60 km long and averages 2 km wide. Its deepest point is approximately 130 m, with sections of the basin averaging

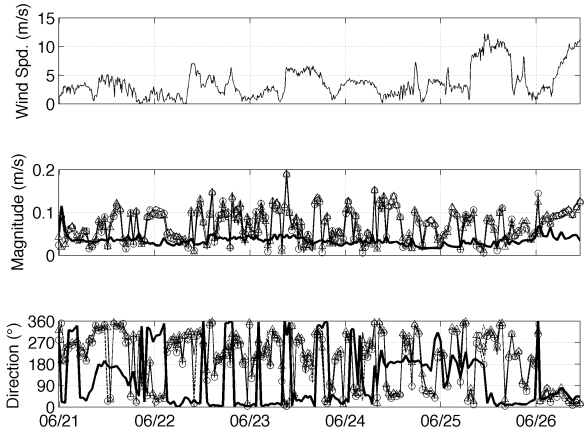

Fig. 8. (top) Wind speed measured 8 m above the lake surface. (middle) Depth averaged magnitude and (bottom) direction estimates from the measured velocities (△), the hydrodynamic model (○), and the rough magnitude estimate (—).

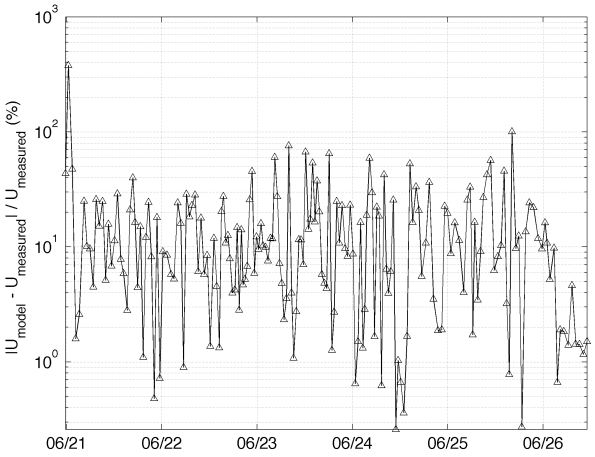

Fig. 9. Percent error between the model and measured velocity depth averaged magnitude.

100 m depth over several kilometer lengths. The sides of the lake are steep with maximum depths being reached within 60-100 meters of shore in many sections. It is well suited for test deployments for this reason.

Flow within the lake is predominantly controlled by surface wind forcing and the baroclinic response to this wind forcing. The density structure of the lake is controlled by temperature, with a thermocline typically established around 10 m depth during the stratified summer season. As wind moves surface water above the thermocline in the direction the wind is blowing, water below the thermocline moves in the opposite direction due to conservation of mass. Velocities above the thermocline are typically much stronger than those below due to the relative thicknesses of the layers. Despite the stronger velocities, the depth averaged velocity should generally be representative of the lower layer because of its larger thickness. Velocity magnitudes are expected to be 0.01-0.10 m/s, with the velocity magnitude dependent on wind speed. Seaglider was deployed for five days and completed a total of 183 dives. Winds were typically light during this period, but increased significantly on the last 1.5 days of the deployment.

Using Eqn. 6, the estimated glider end position obtained from the glider path and the actual glider end position from GPS, depth averaged velocity estimates are obtained from the measured and hydrodynamic model velocities.

Results for the five day deployment from the two depth average velocity estimates and the rough magnitude estimate obtained from the difference between measured and model velocities are shown in Figure 8. Wind speed measured 8 m above the lake surface is also shown.

The measured and model velocity depth averaged estimates agree well in both magnitude and direction. Percent error between the magnitudes of the measured and model velocity estimates, using the measured velocity estimate as a reference is relatively small, with mean and median values of 16.8% and 9.7% respectively (Figure 9).

An independent estimate of the depth averaged velocity is not available for comparison. A rough idea direction can be obtained from available information, however. Surface drift direction should be indicative of the velocity direction above the thermocline. Temperature measurements (not shown) indicate a thermocline depth of 10-15 m in a total depth of 100-130 m, while measurements from a moored profiler (not shown) show magnitudes in the range 0.02-0.10 m/s above the thermocline. The difference between the measured and hydrodynamic model velocity estimates is typically 0.02-0.05 m/s and is a reasonable estimate for velocity magnitudes below the thermocline. Using this information, an estimated depth averaged velocity direction can be determined, which under most conditions will be opposite the direction of surface drift. This estimate, taken simply as a 180° shift in the surface drift direction, is shown in the bottom panel of Figure 8. While not always a good predictor, it works reasonably well and suggests the depth averaged estimates are valid.

V. Conclusion

An acoustic current profiler, the Nortek AD2CP-Glider, was integrated into the science payload of the iRobot Seaglider. The AD2CP-Glider measures a combination of Seaglider velocity and the water velocity. By making certain assumptions, the velocity measurements can be processed to yield an estimate of depth averaged velocity as well as providing horizontal location information to supplement the vertical position information obtained from a pressure sensor.

The AD2CP-Glider measured velocities are a combination of the water and glider velocity, free of any assumptions on how the glider and flow interact. The AD2CP-Glider measurements also provide estimates of the glider velocity in regions where a hydrodynamic model has problems, such as when leaving or returning to the surface or during the dive

apogee. This improves estimates of glider position when using dead reckoning navigation by eliminating gaps in the velocity record. The AD2CP-Glider also measures the combined lateral glider velocity and water velocity, allowing for some inefficiencies in the transfer of momentum to the glider by the flow.

The start and end periods are problematic in dead reckoning (and in eventually estimating a depth averaged or water velocity profile). At the surface, a reasonable estimate of the glider's drift velocity is obtained from GPS positions. Once the glider leaves the surface and before it reaches D_FLARE where it obtains its optimal pitch angle, it is no longer drifting, but actively controlling its buoyancy and pitch. In this region the surface drift velocity is not a good representation of the glider velocity. For instance, the surface drift has a zero vertical velocity component while the actual glider vertical velocity is negative.

Because dead reckoning depends on accurate estimates of velocity to propagate a known position forward, the rapidly changing ambient conditions and glider state (i.e. it's attitude and velocity) in the surface region necessitate a different measurement strategy than mid-water column where the glider is in a more stable environment and operating regime. Similarly, the dive apogee, while not experiencing as varied ambient velocities, has a changing glider state which would benefit from a different sampling strategy than used during the dive and climb phases.

In addition to the position information obtained from the AD2CP velocity record, depth averaged velocity and direction estimates are calculated from the difference in actual and estimated end positions. Because the AD2CP-Glider measured velocities make no assumptions about the interaction of the glider with the flow, they provide a small improvement over a hydrodynamic model of glider flight when estimating depth averaged velocity. Neither velocity estimate is able to provide exact position information without further processing and the incorporation of external references.

While the depth averaged velocity is the simplest data product available from a glider mounted current profiler. The ultimate goal of this collaboration is to generate profiles of water velocity with depth from the measurements. There are several methods available to obtain velocity profiles from measured velocity data [6]–[8], but they all benefit from a high quality estimate of the depth averaged velocity.

Ongoing work by iRobot has led to several advances in how Seaglider flies, allowing a constant ascent angle until the glider reaches the surface and a new operating mode where pitch and heading are maintained to optimize AD2CP-Glider measurements (i.e. it minimizes changes in pitch and roll). These improvements and changes to the AD2CP sampling for different portions of the dive should continue improvement in both navigation and water velocity measurement.

REFERENCES

[1] C. Eriksen, T. Osse, R. Light, T. Wen, T. Lehman, P. Sabin, J. Ballard, and A. Chiodi, "Seaglider: A long-range autonomous underwater vehicle for oceanographic research," *IEEE J. Ocean. Eng.*, vol. 26, no. 4, pp. 424–436, 2001.

[2] A. Lohrmann, R. Cabrera, G. Gelfenbaum, and J. Haines, "Direct measurements of reynolds stress with an acoustic doppler velocimeter," in *Current Measurement, 1995., Proceedings of the IEEE Fifth Working Conference on*, feb 1995, pp. 205 –210.

[3] R. E. Todd, D. L. Rudnick, M. R. Mazloff, R. E. Davis, and B. D. Cornuelle, "Poleward flows in the southern California Current System: Glider observations and numerical simulation," *Journal of Geophysical Research*, vol. 116, no. C2, Feb. 2011.

[4] K. Theriault, "Incoherent multibeam doppler current profiler performance: Part i–estimate variance," *Oceanic Engineering, IEEE Journal of*, vol. 11, no. 1, pp. 7 – 15, jan 1986.

[5] A. Lohrmann and B. Hackett, "High resolution measurements of turbulence, velocity and stress using a pulse-to-pulse coherent sonar," *J. Atmos. Oceanic Tech.*, vol. 7, no. 1, pp. 19–37, 1990.

[6] J. Fischer and M. Visbeck, "Deep velocity profiling with self-contained adcps," *J. Atmos. Oceanic Tech.*, vol. 10, no. 5, pp. 764–773, 1993.

[7] M. Visbeck, "Deep velocity profiling using lowered acoustic doppler current profilers: Bottom track and inverse solutions*," *J. Atmos. Oceanic Tech.*, vol. 19, pp. 794–807, 2002.

[8] M. Stanway, "Water profile navigation with an acoustic doppler current profiler," in *OCEANS 2010 IEEE - Sydney*, may 2010, pp. 1 –5.